Supporting Information

Activation of molecular oxygen by a metal-organic framework with open 2,2'-bipyridine for selective oxidation of saturated hydrocarbons

Jilan Long,[a] Liming Wang,[a] Xingfa Gao,[b] Cuihua Bai,[a] Huanfeng Jiang[a] and Yingwei Li*,[a]

[a] *School of Chemistry and Chemical Engineering, South China University of Technology, Guangzhou 510640, China.*

[b] *CAS Key Laboratory for Biomedical Effects of Nanomaterials and Nanosafety, Institute of High Energy Physics, Chinese Academy of Sciences, Beijing 100049, China.*

* To whom correspondence should be addressed. E-mail: liyw@scut.edu.cn

This PDF file includes:

Experimental

All chemicals were purchased from commercial sources (Sigma-Aldrich, Alfa Aesar, and others). All solvents were analytical grade and distilled prior to use. $AlCl_3 \cdot 6H_2O$ and 2,2'-bipyridine-5,5'-dicarboxylic acid were purchased from different chemical companies.

1. Catalyst Preparation

MOF-253 was prepared from hydrothermal reaction of $AlCl_3 \cdot 6H_2O$ (151 mg, 0.625 mmol), 2,2'-bipyridine-5,5'-dicarboxylic acid (153 mg, 0.625 mmol), and 10 mL N,N'-dimethylformamide (DMF) at 130 °C for 24 h. The resulting white microcrystalline powder was then filtered and washed with DMF thoroughly. The solid was washed with methanol via soxhlet extraction for 24 h, and then was collected by filtration and finally dried at 200 °C under vacuum for 12 h. Elemental analysis (%): calcd for $C_{12}H_7AlN_2O_5 \cdot 0.5H_2O$: Al, 9.14; C, 48.82; H, 2.74; N, 9.49. Found: Al, 8.98; C, 48.90; H, 2.56; N, 9.53.

2. Characterization

Powder X-ray diffraction patterns of the samples were obtained on a Rigaku diffractometer (D/MAX-IIIA, 3 kW) using Cu Kα radiation (40 kV, 30 mA, $\lambda = 0.1543$ nm). BET surface area and pore size measurements were performed with N_2 adsorption/desorption isotherms at 77 K on a Micromeritics ASAP 2020 instrument. Before the analysis, samples were evacuated at 150 °C for 12 h. Atomic absorption spectroscopy (AAS) was obtained on a HITACHI Z-2300 instrument. Solid samples were digested with chloroazotic acid before the AAS analysis. Infrared (IR) spectrum was recorded (4000-400 cm^{-1}) on a Nicolet iS10 Fourier Transform Infrared Spectrometer.

3. Catalytic Reactions

3.1 General procedure for cyclohexane oxidation

The oxidation of cyclohexane was carried out in a 50 mL Teflon-lined stainless steel autoclave equipped with a pressure gauge and a magnetic stirrer. The autoclave was connected to an oxygen

cylinder, and the reaction pressure was controlled with a precise gas regulator, so that oxygen of fixed pressure could be supplied continuously. Typically, 20 mL of cyclohexane and catalyst (0.09 mol%) were loaded into the reactor. The autoclave was sealed, cooled to 0 °C by placing it to an ice bath, and purged several times with O_2 to remove the air. Then the reactor was loaded in an oil bath that was preheated to the target temperature. The temperature was controlled by a temperature controller, and the temperature fluctuation of the oil bath was ± 0.1 °C. A thermocouple was placed inside the reactor to measure the temperature of the reaction mixture. Once the solution temperature reached 150 °C, the reactor was pressurized with O_2. After the reaction, the autoclave was cooled to 0 °C in an ice bath. The gaseous products were collected with a gas bag, and subsequently analyzed by a GC equipped with a TCD detector and a packed column (Carbon molecular sieve TDX-01). The GC traces of the gaseous samples indicate that no gaseous product was produced in the oxidation reactions. The catalyst was separated from the solution by centrifugation, and then washed with diethyl ether. The reaction products were quantified and identified by GC-MS analysis (Shimadzu GCMS-QP5050A equipped with a 0.2 mm × 0.25 μm × 30 m HP-5 capillary column). The main products and by-products include cyclohexanone, cyclohexanol, formic acid cyclohexyl ester (selectivity <13%), organic acids (e.g. formic acid and valeric acid (selectivity <5%), and adipic acid (selectivity <3%)), and cyclohexyl hydroperoxide, etc. The carbon balance values calculated for all the reaction tests were around 100% (100 ± 2.0%).

3.2 Pretreatment of MOF-253 in O_2 before the addition of cyclohexane

A mixture of MOF-253 (50 mg) in acetonitrile (2 mL) was added into the autoclave. The reactor was pressurized with O_2 (1.0 MPa) and heated at 150 °C for 0.5 hours. Then, cyclohexane (20 mL) was injected into the mixture by a high-pressure pump.

3.3 Recycling of the MOF-253 catalyst

The recyclability of the MOF-253 catalyst was tested for cyclohexane oxidation under the investigated reaction conditions as described above. Scaled-up experiments were performed to take catalyst loss during handling into account. Slightly scaling-up the experiments in the autoclave system was found not to affect the reaction outcomes. Each time, the catalyst was separated from the reaction mixture by centrifugation at the end of catalytic reaction, thoroughly washed with ethyl acetate and acetonitrile, and then evacuated at 100 °C overnight. The dried powder was reused as catalyst for a new experiment that was scaled according to the amount of recovered catalyst. Identical conversion was obtained on reuse of the MOF-253 catalyst for up to five runs (Table S4). PXRD shows that the crystalline structure of the catalyst mostly remained unchanged (Figure S3). Moreover, no metal (i.e. Al) was observed to have leached into the liquid phase. These results indicate that the catalyst was stable and reusable under the investigated conditions.

3.4 Leaching test

To study the leaching of Al during the reaction, after reaction, the mixture was hot filtrated under vacuum. The solid was washed with acetic ether and acetonitrile. The decanted liquid was analyzed for leached metals using atomic absorption spectroscopy and metal concentrations were below the detection limit.

4. Density Functional Theory Calculations

Geometry optimizations were performed using the B3LYP[S1-S3] method in conjunction with the 6-31G(d,p)[S4-S6] basis set, followed by frequency calculations at the same level of theory. No imaginary frequencies were found, which confirmed the optimized structures to be local energy minima. The HOMO, LUMO energies, and HOMO-LUMO gaps were obtained by single-point energy calculations using the B3LYP with a larger basis set, 6-311+G(d,p).[S7-S11] All calculations were done using the Gaussian 09 program.[S12]

References

(S1) Becke, A. D. *Phys. Rev. A* **1988**, *38*, 3098.

(S2) Becke, A. D. *J. Chem. Phys.* **1993**, *98*, 5648.

(S3) Lee, C.; Yang, W.; Parr, R. G. *Phys. Rev. B* **1988**, *37*, 785.

(S4) Hehre, W. J.; Ditchfield, R.; Pople, J. A. *J. Chem. Phys.* **1972**, *56*, 2257.

(S5) Hariharan, P. C.; Pople, J. A. *Mol. Phys.* **1974**, *27*, 209.

(S6) Francl, M. M.; Pietro, W. J.; Hehre, W. J.; Binkley, J. S.; Gordon, M. S.; DeFrees, D. J.; Pople, J. A. *J. Chem. Phys.* **1982**, *77*, 3654.

(S7) Krishnan, R.; Binkley, J. S.; Seeger, R.; Pople, J. A. *J. Chem. Phys.* **1980**, *72*, 650.

(S8) McLean, A. D.; Chandler, G. S. *J. Chem. Phys.* **1980**, *72*, 5639.

(S9) Clark, T.; Chandrasekhar, J.; Spitznagel, G. W.; Schleyer, P. v. R. *J. Comput. Chem.* **1983**, *4*, 294.

(S10) Hariharan, P. C.; Pople, J. A. *Theor. Chim. Acta* **1973**, *28*, 213.

(S11) Frisch, M. J.; Pople, J. A.; Binkley, J. S. *J. Chem. Phys.* **1984**, *80*, 3265.

(S12) Frisch, M. J.; Trucks, G. W.; Schlegel, H. B.; Scuseria, G. E.; Robb, M. A.; Cheeseman, J. R.; Scalmani, G.; Barone, V.; Mennucci, B.; Petersson, G. A.; Nakatsuji, H.; Caricato, M.; Li, X.; Hratchian, H. P.; Izmaylov, A. F.; Bloino, J.; Zheng, G.; Sonnenberg, J. L.; Hada, M.; Ehara, M.; Toyota, K.; Fukuda, R.; Hasegawa, J.; Ishida, M.; Nakajima, T.; Honda, Y.; Kitao, O.; Nakai, H.; Vreven, T.; Montgomery, Jr., J. A.; Peralta, J. E.; Ogliaro, F.; Bearpark, M.; Heyd, J. J.; Brothers, E.; Kudin, K. N.; Staroverov, V. N.; Kobayashi, R.; Normand, J.; Raghavachari, K.; Rendell, A.; Burant, J. C.; Iyengar, S. S.; Tomasi, J.; Cossi, M.; Rega, N.; Millam, J. M.; Klene, M.; Knox, J. E.; Cross, J. B.; Bakken, V.; Adamo, C.; Jaramillo, J.; Gomperts, R.; Stratmann, R. E.; Yazyev, O.; Austin, A. J.; Cammi, R.; Pomelli, C.; Ochterski, J. W.; Martin, R. L.; Morokuma, K.; Zakrzewski, V. G.; Voth, G. A.; Salvador, P.; Dannenberg, J. J.; Dapprich, S.; Daniels, A. D.; Farkas, O.; Foresman, J. B.; Ortiz, J. V.; Cioslowski, J.; Fox, D. J. Gaussian, Inc., Wallingford CT, 2009.

Table S1. Previous literature results on liquid-phase cyclohexane oxidation using dioxygen.

Catalyst	Temperature/ pressure/time	Solvent	Promoter	Con. (%)	Sel. (%)[a]		Ref.
					C=O	C-OH	
Ag/MCM-41	155 °C 1.4 MPa O_2 3 h	–	–	10.7	45.3	38.1	S13
Au/ZMS-5	150 °C 1 MPa O_2 4 h	–	–	16	67	25	S14
Au/MCM-41	150 °C 1 MPa O_2 6 h	–	–	19	73	21	S15
Au/Al_2O_3	150 °C 1.5MPa O_2 3 h	–	–	12.6	32.1	52.6	S16
Au/F-SBA-15-Co	150 °C 1 MPa O_2 2 h	–	–	16.6	92.4		S17
Au/MPTMS	150 °C 1 MPa O_2 2 h	–	–	21.5	56	34.4	S18
CNT	120 °C 1.5 MPa O_2 8 h	Acetone	Cyclohexanone	34.3	22.0	18.4	S19
GSCN-20	150 °C 1 MPa O_2 4 h	CH_3CN	–	12	94	6	S20
Cu/SBA-15	120 °C 1 MPa O_2 5 h	–	–	9.5	49.4	31.8	S21
FeAlPO-5	130 °C 1.5 MPa air 24 h	–	TBHP	19.8	32.5	21.7	S22
Co/ZSM-5	100 °C 1 MPa O_2 4 h	–	–	7.5	46	46.4	S23
Ce/AlPO-5	140 ℃ 0.5 MPa O_2 4 h			13	50	42	S24

[a] C=O indicates cyclohexanone, and OH denotes cyclohexanol.

References

(S13) H. Zhao, J. Zhou, H. Luo, C. Zeng, D. Li, Y. Liu, *Catal. Lett.* **2006**, *108*, 49.

(S14) R. Zhao, D. Ji, G. Lv, G. Qian, L. Yan, X. Wang, J. Suo, *Chem. Commun*. **2004**, 904.

(S15) G. Lv , R. Zhao, G. Qian, Y. Qi, X. Wang, J. Suo, *Catal. Lett.* **2004**, *97*, 115.

(S16) L. Xu, C. He, M. Q. Zhu, S. Fang, *Catal. Lett.* **2007**, *114*, 202.

(S17) P. Wu, P. Bai, K. P. Loh, X. S. Zhao, *Catal. Today* **2010**, *158*, 220.

(S18) P. Wu, P. Bai, Z. Lei, K. P. Loh, X. S. Zhao, *Micropor. Mesopor. Mat.* **2011**, *141*, 222.

(S19) H. Yu, F. Peng, J. Tan, X. Hu, H. Wang, J. Yang, W. Zheng, *Angew. Chem. Int. Ed.* **2011**, *50*, 3978.

(S20) X.-H. Li, J.-S. Chen, X. Wang, J. Sun, M. Antonietti, *J. Am. Chem. Soc.* **2011**, *133*, 8074.

(S21) J. Gu, Y. Huang, S. P. Elangovan, Y. Li, W. Zhao, I. Toshio, Y. Yamazaki, J. Shi, *J. Phys. Chem. C* **2011**, *115*, 21211.

(S22) R. Raja, G. Sankar, J. M. Thomas, *J. Am. Chem. Soc.* **1999**, *121*, 11926.

(S23) H. X. Yuan , Q. H. Xia , H. J. Zhan, X. H. Lu, K. X. Su, *Appl. Catal. A: Gen.* **2006**, *304*, 178.

(S24) R. Zhao, Y. Wang, Y. Guo, Y. Guo, X. Liu, Z. Zhang, Y. Wang, W. Zhan, G. Lu, *Green Chem.* **2006**, *8*, 459.

The effect of possible metal impurities present in the reaction system on the oxidation was carefully examined. First, we analyzed the fresh MOF-253 catalyst and the reaction mixture after the blank run (without catalyst) using atomic absorption spectroscopy (AAS). Indeed, 0.03–0.15 ppm of Fe, Cr, Mn, Ni, and Zn metal species were detected in the MOF and the reaction solution (Table S2). However, the use of 100–1,000 times these quantities of various metal salts as catalysts in the reaction did not obviously enhance the reaction rate of the blank run (Table S3). Moreover, we also found that the addition of traces of these metal ions (e.g. Co^{2+}, Mn^{2+}) to the MOF reaction system did not improve the reaction outcome, and in some cases the reaction efficacy was slightly reduced (Table S3). On the other hand, the use of different batches of MOF-253 catalysts using various sources of $AlCl_3 \cdot 6H_2O$ and 2,2'-bipyridine-5,5'-dicarboxylic acid did not dramatically affect the reaction results. We also reproduced the key experiments with new reactors, further confirming the reliability of our observations.

Table S2. AAS analysis of various metals in catalyst and the liquid mixture after blank run.

Element	Catalyst	Solution[a]
Fe	n.d.	0.1400
Cr	n.d.	0.1200
Cu	0.0346	n.d.
Mn	n.d.	0.0311
Zn	0.0417	0.0429
Ni	n.d.	0.0910
Co	n.d.	n.d.
Pd	n.d.	n.d.

Unit: mg/kg (ppm).

[a] A blank run with cyclohexane and O_2 without the addition of any catalyst.

Table S3. Results of the oxidation of cyclohexane in the absence of solvent with O_2[a]

Entry	Catalyst	Metal content (ppm)[b]	Con. (%)	Yield of KA-oil (%)
1	$Fe(acac)_3$	15	0.05	0.03
2	$Cr(OAc)_3$	15	0.08	0.05
3	$Cu(OAc)_2$	15	0.10	0.09
4	$Mn(OAc)_2$	20	0.12	0.02
5	$Zn(acac)_2$	10	0.06	0.02
6	$Ni(acac)_2$	20	-	-
7	$Co(acac)_2$	20	0.06	-
8	$Pd(OAc)_2$	20	-	-
9[c]	$Mn(OAc)_2$ + MOF-253	20	56.6	45.5
10[c]	$Co(acac)_2$ + MOF-253	20	58.1	46.5

[a] Reaction conditions: cyclohexane (20 mL), O_2 (1.0 MPa), 4 h. [b] Metal content of the added metal complexes in the reaction solution. [c] MOF-253 (50 mg).

Table S4. Reusability of the MOF-253 catalyst in the oxidation of cyclohexane[a]

Use	Con. (%)	Sel. (%)		Yield of KA-oil (%)
		C=O	OH	
1	59.9	48.1	32.1	48.0
2	56.9	47.0	34.2	46.2
3	57.8	49.6	31.6	46.9
4	59.0	49.1	31.5	47.6
5	58.8	49.4	32.0	47.9

[a] Reaction conditions: cyclohexane (20 mL), MOF-253 (0.09 mol%), 150 °C, O_2 (1.0 MPa), 4 h.

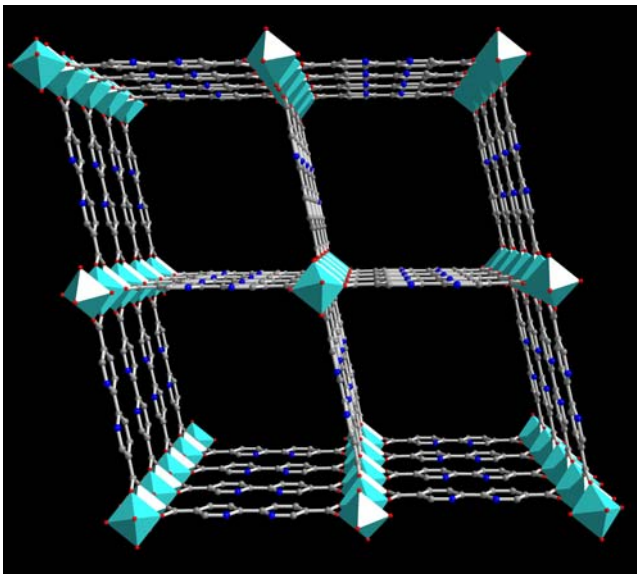

Figure S1. Representative structure of MOF-253. Cyan octahedra represent Al atoms. Oxygen, red; nitrogen, blue; carbon, gray. H atoms are omitted for clarity.

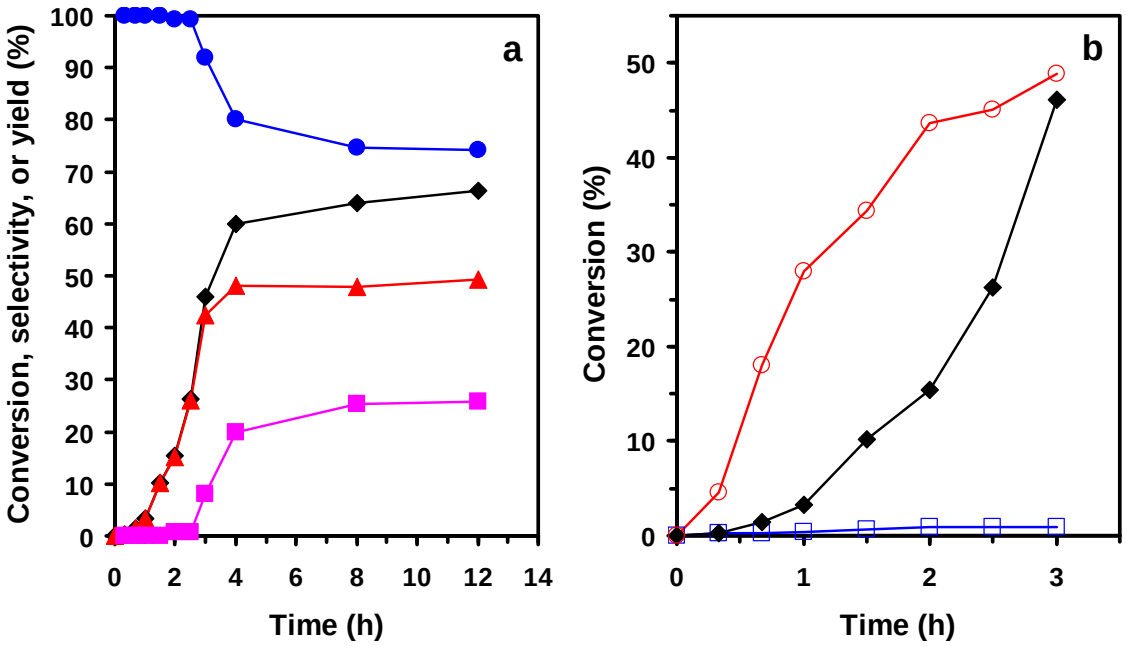

Figure S2. Cyclohexane conversion, product selectivity, and yield as a function of time: cyclohexane (20 mL), MOF-253 (0.09 mol%), O_2 (1.0 MPa), 150 °C. Symbols: ◆, conversion; ●, selectivity to KA-oil; ■, selectivity to byproducts; ▲, yield of KA-oil; □, cyclohexane conversion in the presence of p-benzoquinone; ○, cyclohexane conversion after pre-activation.

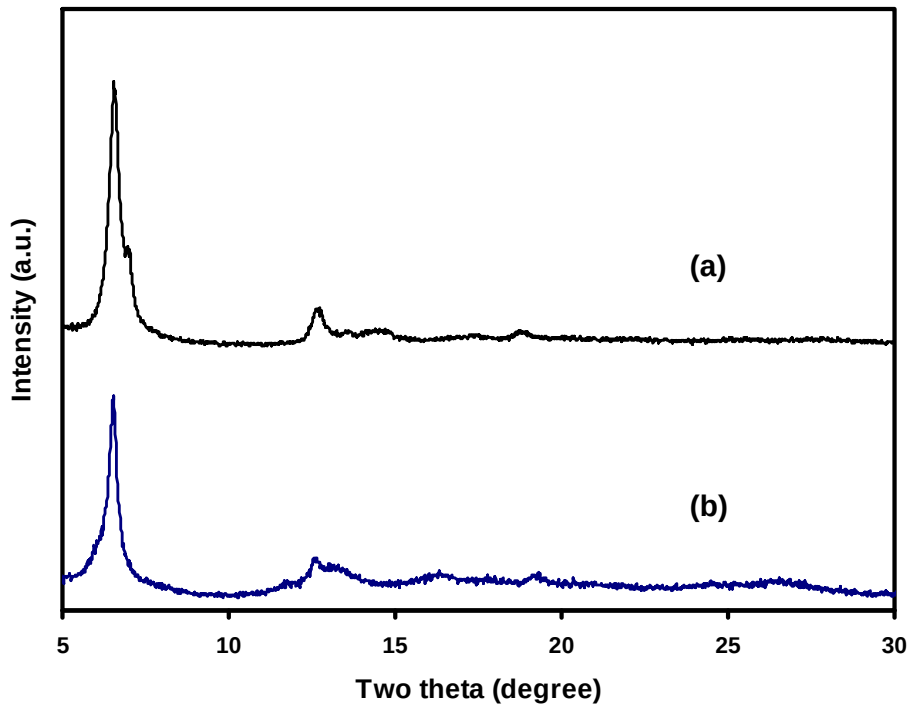

Figure S3. Powder XRD patterns for MOF-253 samples recorded before (a) and after catalytic reaction (b).

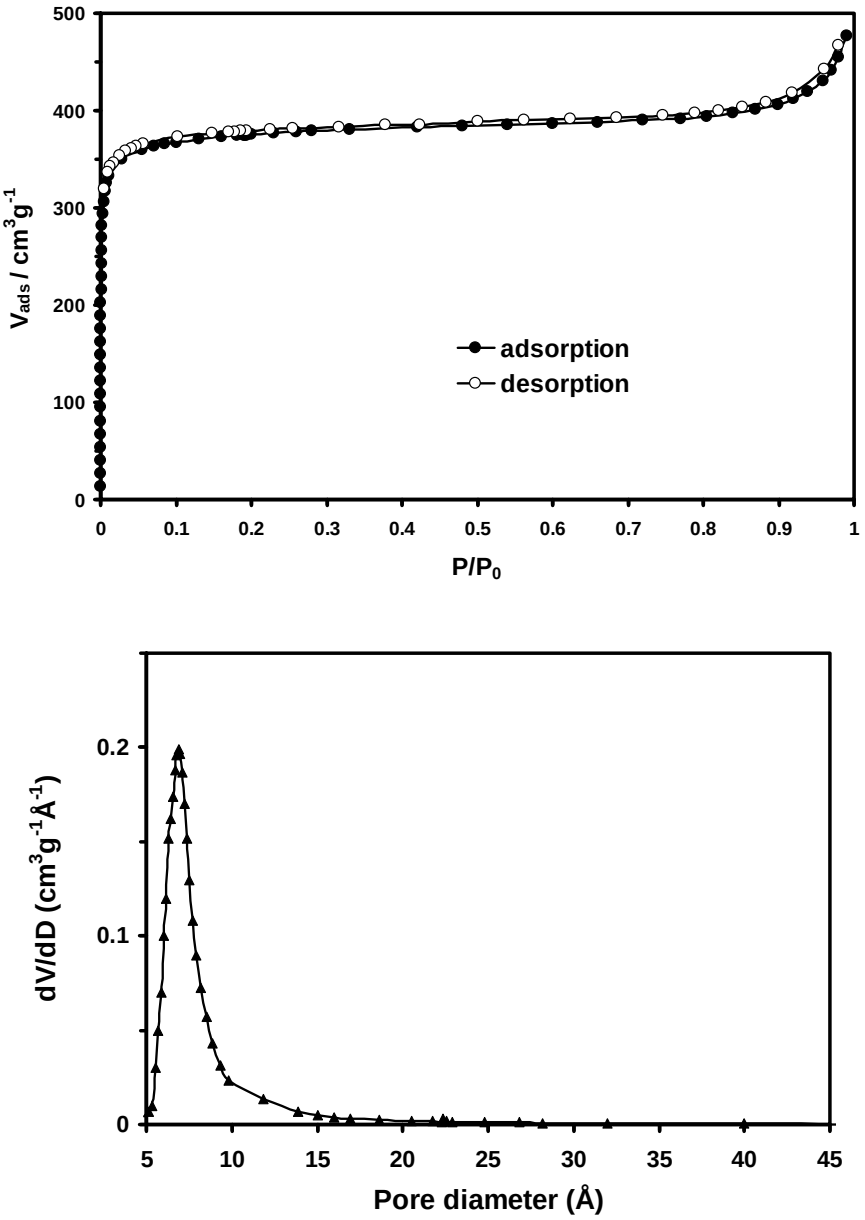

Figure S4. Nitrogen isotherms at 77 K (top) and micropore size distribution (bottom) of MOF-253.

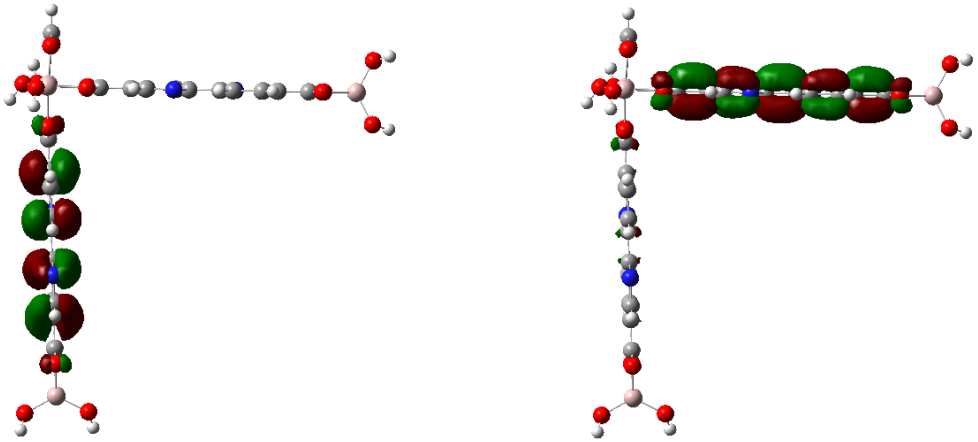

Figure S5. The diagrams of HOMO (left) and LUMO (right) with isovalues of 0.03, calculated at the B3LYP/6-311+G(d,p)//B3LYP/6-31G(d,p) level of theory.

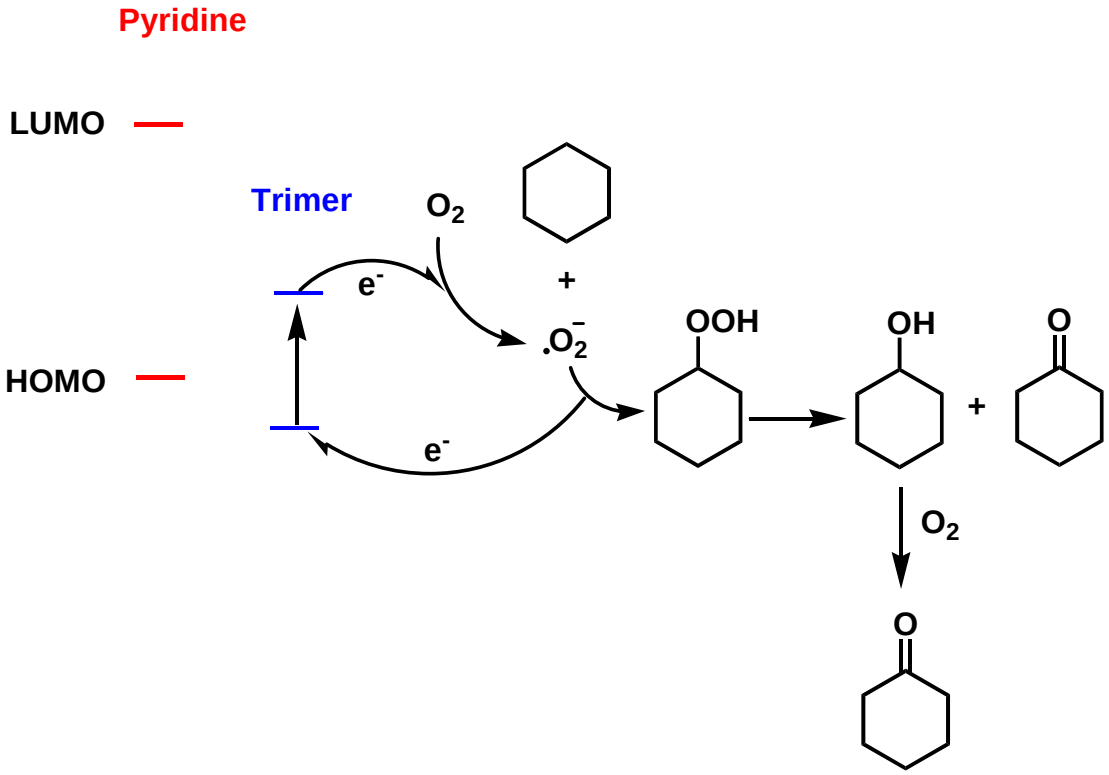

Figure S6. Schematic representation of the mechanism for cyclohexane aerobic oxidation.

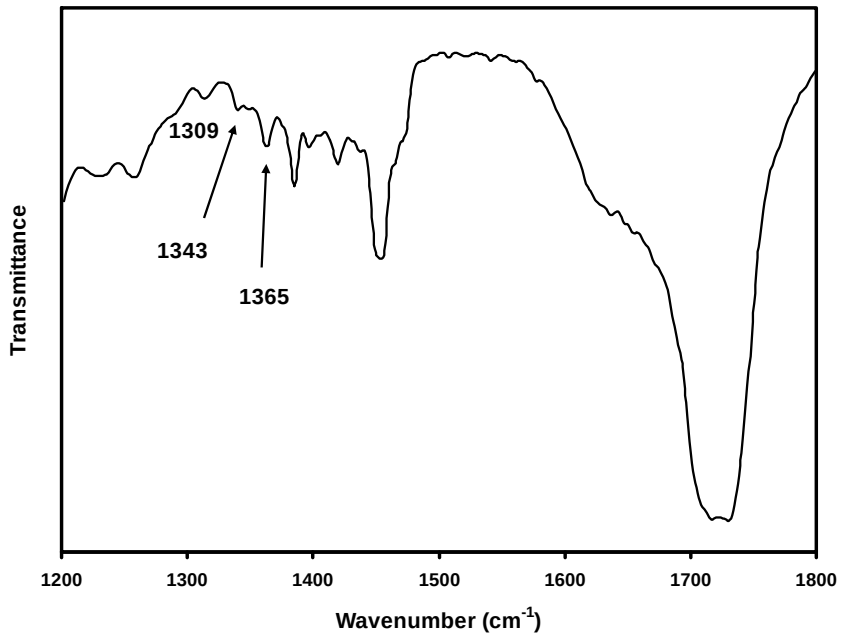

Figure S7. IR spectrum of the solution after 4 h of reaction of cyclohexane with oxygen using MOF-253 as catalyst. The peaks at 1365, 1343, and 1309 cm^{-1} can be assigned to the vibrational modes of cyclohexyl hydroperoxide (Sun, H., Blatter, F., and Frei, H., *J. Am. Chem. Soc.* **1996**, *118*, 6873).

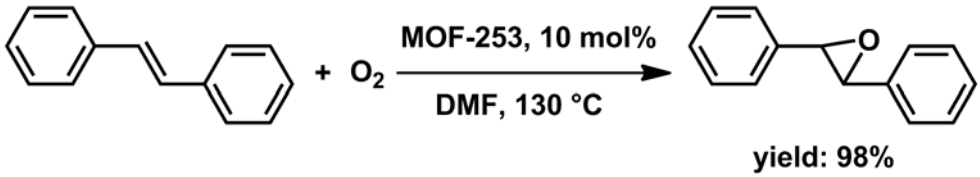

Figure S8. Oxidation of (E)-1,2-diphenylethene. Reaction conditions: (E)-1,2-diphenylethene (0.5 mmol), MOF-253 (10 mol%), DMF (2 mL), 130 °C, 1.0 MPa of O_2, 10 h.